Initiation of Spontaneous Epileptiform Events in the Rat Neocortex In Vivo

Hong-tao Ma,[2,1] Cai-hong Wu,[2] Jian-young Wu[1]

[1]*Department of Physiology and Biophysics, Georgetown University, Washington DC, 20057-1421; and* [2]*Department of Physiology and Biophysics, College of Life Science, Peking University, Beijing, 100871, Peoples Republic of China*

Ma, Hong-tao, Cai-hong Wu, and Jian-young Wu. Initiation of spontaneous epileptiform events in the rat neocortex in vivo. *J Neurophysiol* 91: 934–945, 2004. First published October 8, 2003; 10.1152/jn.00274.2003. We used voltage-sensitive dye imaging to visualize the distribution of initiation sites of the spontaneous interictal-like spikes (sISs) in rat neocortex, in vivo, induced by bicuculline or picrotoxin over the exposed cortex. The initiation site was small (approximately 200 μm diam). On average each initiation site initiated 2.0 ± 0.8 sISs (9 animals, 499 sISs, 251 sites). This is significantly different from that in neocortical slices, where each initiation site initiated 30–100 sISs. The initiation sites were not randomly distributed. The distance between two consecutive sites tended to be either <800 or >1200 μm, suggesting a temporal "suppression annulus" surrounding each initiation site. Within the annulus, the likelihood for initiating the next sIS was reduced. Suppression annulus did not have a noticeable change in the presence of $GABA_b$ antagonist, suggesting it did not depend on the $GABA_b$ inhibition. We also applied bicuculline locally to a spot of 800×800 μm^2 for approximately 45 min. During this period approximately 1000 sISs occurred within the spot. Bicuculline or picrotoxin was then applied to the entire craniotomy window. The pretreatment created an obvious cluster of initiation sites. Around this cluster, the suppression annulus became obvious in individual animals. Our results suggest that, in disinhibited cortex, epileptiform events were initiated from small sites. The initiation sites may cluster in an area with increased local activity. Surrounding each initiation site there may be a temporal suppression annulus.

INTRODUCTION

Epileptiform activity can be initiated from cortical structures (McNamara 1994; Traub et al. 1994), suggesting that intrinsic characteristics of the cortex contribute to the initiation of epileptiform activity. The interictal spike (IS) is the simplest identifiable unit of epileptiform activity in the CNS (McCormick and Contreras 2001). In several human epileptic conditions, the spontaneous IS (sIS) represents the electrographic hallmark of an active epileptic focus (Ajmone 1978; Jefferys 1990). Focal application of convulsants onto cortex in vivo can induce sISs (Federico et al. 1994; Lebovitz 1975; Schwartz and Bonhoeffer 2001), suggesting that the generation of a sIS is a local event. In vitro experiments have demonstrated that a small piece of neocortical tissue perfused with a convulsant is enough to generate sISs and organized seizure-like activities (Anderson et al. 1986; Flint and Connors 1996; Silva et al. 1991; Wong and Prince 1990). Voltage-sensitive dye and optical imaging have further shown that the initiation site for a sIS can be smaller than $0.4 \times 0.4 \times 0.4$ mm^3 in neocortical slices (Tsau et al. 1998, 1999), suggesting that generating a sIS

only requires a small group of neurons. A rat neocortical slice is about $4 \times 2 \times 0.4$ mm^3 and this volume may contain tissue for approximately 50 potential initiation sites. In a slice of this size, the sISs are not generated randomly from all potential initiation sites. Instead, the majority of sISs are generated from only a few initiation sites, and one or two initiation sites may become dominant for a period of time (Tsau et al. 1998). An intact cortex in vivo may contain more potential initiation sites than a slice in vitro. It is not known, however, whether sISs are also initiated from dominant sites in vivo.

In this report, we use voltage-sensitive dye (VSD) imaging to map the sIS initiation sites in vivo, in a cortical region disinhibited by bicuculline or picrotoxin. This region (5 mm diam) has the potential to host many initiation sites.

Optical imaging with VSD offers both high spatial and temporal resolutions. The VSD signal is fast enough to follow neuronal action potentials and is linearly related to the transmembrane potential (Ross et al. 1977). When imaging cortical tissue, each optical detector receives light from thousands of neurons and the VSD signal is the linear summation of the membrane potentials of these neurons (Cohen and Salzburg 1978). Volume conductance effect in the tissue does not influence this signal, so the method can be used to pinpoint the small neuronal cluster that initiates a sIS. Other methods are limited for our purpose. The spatial resolution of a field potential electrode array is limited by the volume conductance effect (Buzsáki and Traub 1997). Extracellular single-unit electrodes have good spatial and temporal resolution (Goldensohn and Salaza 1986), but it is difficult to place multiple electrodes in a small area to locate the sIS initiation site. Since the initiation of a sIS occurs within a few milliseconds (Demir et al. 1999; Tsau et al. 1998), functional MRI (fMRI), PET, single-photon emission computed tomography (SPECT), and optical imaging of intrinsic signals do not have adequate temporal resolution (Bonhoeffer and Grinvald 1996; Duncan 1997).

In vivo VSD imaging is still a difficult technique because heartbeat and blood perfusion introduce large artifacts. In this report we used a popular dye, RH-795 (Grinvald et al. 1994); the pulsation artifacts are about the same size as the sIS signal (however, new dyes may improve the signal-to-noise ratio (Shoham et al. 1999). We used ECG-triggered subtraction to eliminate the pulsation artifact. The VSD signal of sISs was large, allowing us to separate the artifact and to locate the initiation sites without averaging.

While this paper was in preparation, Miyakawa and colleagues published a study using VSD imaging to examine the

---

0022-3077/04 $5.00 Copyright © 2004 The American Physiological Society

distribution of sIS initiation sites (Miyakawa et al. 2003). They have shown that the initiation sites of sISs were "neither unique nor randomly" distributed in the cortex. Here we report two observations on the distribution of the initiation sites: the suppression annulus surrounding each initiation site and the clustering of initiation sites related to the activity history. Our results suggest that the distribution of initiation sites may have unique spatiotemporal characteristics.

METHODS

Preparation

Adult male Sprague–Dawley rats (250–350g) were used in all the experiments. All surgical procedures were approved by the Georgetown University Animal Care and Use Committee following National Institutes of Health guidelines. The animals were initially anesthetized to surgical level with ip injections of urethane (1.25 g/kg). Additional doses (10% of initial dose) were applied by ip injection to maintain the anesthetic level when necessary. A regulated heating pad was used to maintain the body temperature at 38°C. The head was fixed in a stereotaxic frame. A craniotomy window of approximately 7 mm diam was opened over the right hemisphere. The location of the craniotomy window is shown in Fig. 1A. A well was built around the craniotomy window with dental acrylic. Dura over the window was

removed and the brain was covered with artificial cerebral spinal fluid (ACSF). The ACSF contained (in mM) 132 NaCl, 3 KCl, 2 $CaCl_2$, 2 $MgSO_4$, 1.25 NaH_2PO_4, 26 $NaHCO_3$ and 10 dextrose, bubbled with 95% O_2–5% CO_2 to maintain the pH at 7.4 before application to the cortex. The dye, RH-795 solution (Molecular Probes, 0.6 mg/ml in ACSF), was applied to the exposed cortex for approximately 45 min (London et al. 1989). After staining, the cortex was washed with dye-free ACSF for approximately 15 min.

During imaging the exposed cortex was covered with bicuculline (1 mM) or picrotoxin (1 mM) solution in ACSF. In some experiments 1 mM $GABA_b$ receptor antagonist CGP35348 (Sigma) was added to the bicuculline solution. In another set of experiments (see Fig. 8), bicuculline was first applied locally to the cortex with a piece of filter paper (approximately 800×800 μm^2) soaked with 1 mM bicuculline. The cortex was covered with silicon oil (12,500 centistoke) to reduce diffusion when bicuculline was applied locally. After 45 min, the silicon oil was removed and bicuculline or picrotoxin was applied to the entire exposed cortex during imaging.

Recording

A region of cortex (5 mm diam) was imaged by a ×4 macroscope onto a 464-photodiode array (WuTech Instruments, www.wutech.com, available as NeuroPlex by RedshirtImaging, www.redshirtimaging.com) (Fig. 1B). Each diode received signals from an area of 200 μm diam
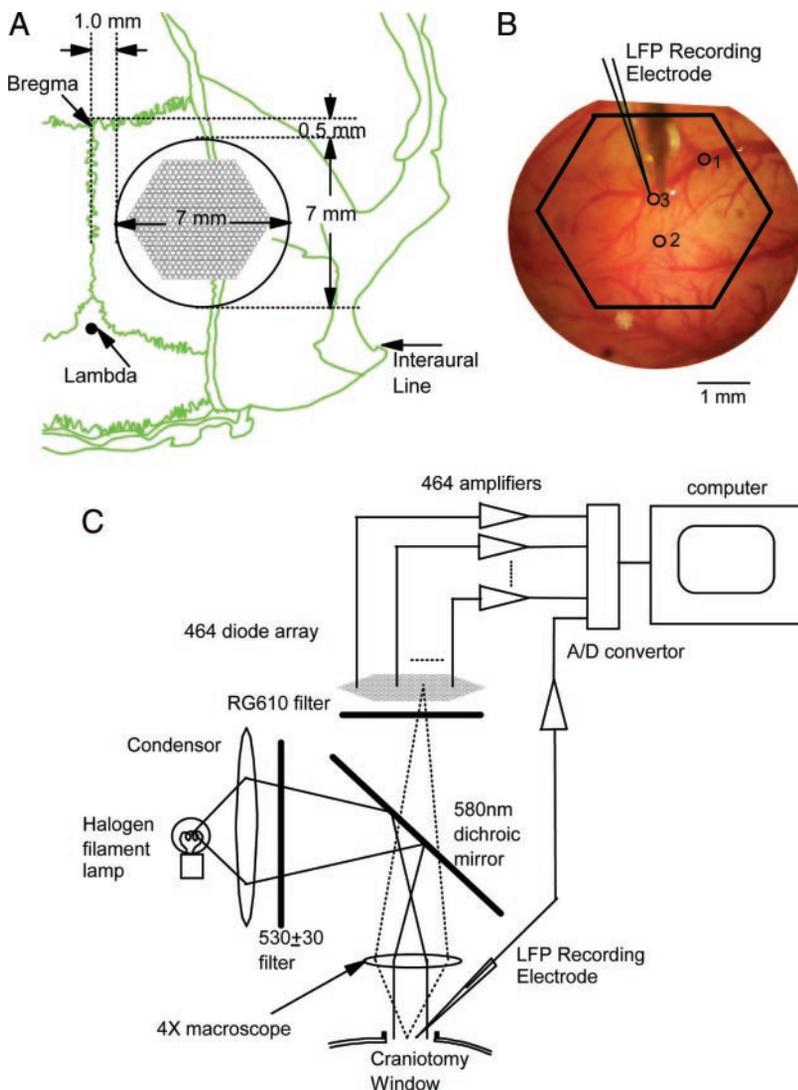

FIG. 1. A: position of the craniotomy window on the skull; green line shows the skull. Craniotomy window (black circle) was created over the right hemisphere. Center of the window was 4.5 mm to the midline and 4 mm posterior to the bregma. The outline of the diode array photodiodes was drawn in the craniotomy window, illustrating the field of view. B: craniotomy window during the experiment, showing the relative locations of the imaging field of view, the field potential electrode, and 3 optical detectors (circles 1, 2, and 3). Traces from the electrode and optical detectors are shown in Fig. 2A. Size of the circles is approximately the same as the cortical area projected to one optical detector on the array. C: schematic drawing of the illumination and recording arrangement. Light from a Tungsten filament lamp (12 V, 100 W, Zeiss) passed through a 530 ± 30 nm filter and reflected via a 580 dichroic mirror onto the cortex (stained with voltage-sensitive dye RH-795). The filament of the lamp was focused onto the back focus plane of the ×4 macroscope to achieve Kohler illumination. Fluorescent light from the stained cortex passed through the dichroic mirror and was filtered by a 610-nm long-pass filter (RG-610) and then formed a real image onto the fiberoptic aperture of the 464-photodiode array. Signals from each photodiode and from the field potential electrode were amplified individually and digitized simultaneously.

(Fig. 1*C*). A tungsten filament lamp (12 V, 100 W, Zeiss) was used for illumination. The light passed through a 530 ± 30 nm interference filter (Chroma Technology) and reflected down onto the cortex via a 580 nm dichroic mirror (Chroma Technology). Kohler illumination was achieved through the macroscope. The fluorescence of the dye (approximately 712 nm) (Takashima et al. 1999) from the stained cortex was focused by the macroscope, filtered by a 610 nm long-pass filter (RG-610, Edmund Scientific), and projected onto the fiber optic aperture of the diode array. The signals from each photodiode were individually amplified with a two-stage amplifier (50 M × 50, 0.2–400 Hz band-pass filtered). The signal was digitized and stored in a personal computer. Data were displayed and analyzed off-line by the NeuroPlex software. For additional information regarding the VSD method, see Wu and Cohen (1993) and Jin et al. (2002).

Local field potential (LFP) was recorded with a ball electrode (Ag–AgCl, approximately 150 μm diam) placed on the cortical surface (Fig. 1*B*). The reference electrode for the LFP was placed in a hole in the bone in front of the craniotomy window.

To reduce floor vibration, a vibration isolation table (Minus-K, www.minusk.com) was used. To reduce the pulsation artifact, in some preparations, the cortex was covered with high viscosity silicon oil (12,500 centistoke) and a cover glass during each imaging trial. The silicon oil was replaced with bicuculline solution between imaging trials.

The total recording time was limited by combined effects of dye bleaching, phototoxicity, and dye wash out (Wu and Cohen 1993; Jin et al. 2002). In one group of five animals, we divided the recording into several (no more than 8) 8-s trials (maxim 64 s of exposure time during a period of 2 h). Usually two to six sISs were recorded in each 8-s trial and 13 to 26 sISs were recorded from each animal. In another group of four animals, experiments were carried out within 40 min to reduce the dye wash out. In this group we had 40-s-long trials and 240 s of total recording time for each animal. Longer single recording trials allowed 80–120 sISs to be recorded from each animal.

Subtraction of pulsation artifact

The dominant source of noise in our measurement was the pulsation artifact associated with the heartbeat. The excitation wavelength of RH-795 overlaps with the light absorption of hemoglobin (Shoham et al. 1999), and the illumination intensity fluctuates following each heartbeat. In our recording, this pulsation artifact had a large amplitude, similar to that of a sIS signal (Fig. 2*A*, *Det 1- 3*). To eliminate this artifact, a subtraction procedure was used off-line in data analysis. An averaged pulsation artifact was obtained by a heartbeat triggered (using the peak of the QRS wave in the ECG) average. During each 8-s trial, there were about 50 heartbeats and we divided the data into about 50 sections, each starting at the time of the QRS peak (Fig. 2*A*). Only 2 to 6 of these approximately 50 sections contained a sIS spike. These sections were defined as the "raw signal" (Fig. 2*B*, *thin solid trace*) and were excluded from the averaging. The sections without sISs were averaged together and defined as "averaged pulsation artifact" (Fig. 2*B*, *dashed trace*). This averaging procedure was applied individually for each optical detector. The averaged pulsation artifact was subtracted from each section of raw signal. After this subtraction the processed signal had a relatively flat base line (Fig. 2*B*, *thick solid trace*).

Locating the sIS initiation sites

After the averaged pulsation artifacts were subtracted from raw VSD signals, the processed signals at different locations during each sIS were normalized to the peak of the signal (Fig. 3*A*). The onset time was defined as the time for the signal to reach half of the peak amplitude of an IS. The location with the earliest onset time was defined as the initiation site (Fig. 3*A*, detector *c*). Pseudocolor images were used to map the initiation site (Fig. 3*B*). To generate a pseudo-
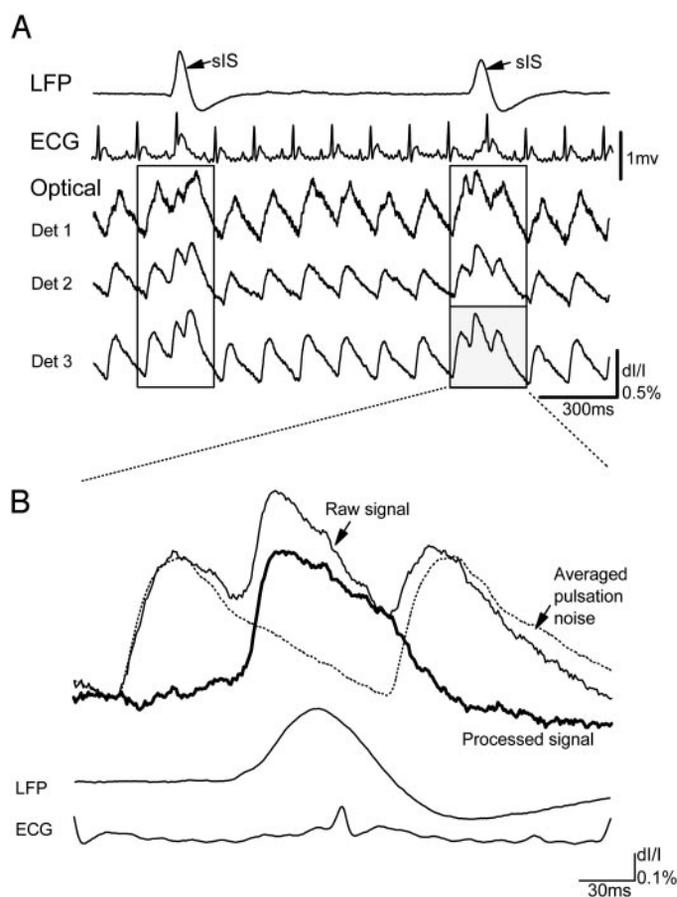

FIG. 2. Heartbeat noise subtraction. *A*: local field potential (LFP), ECG, and optical signals from 3 optical detectors (*Det 1–3*, locations shown in Fig. 1*B*). In this time period, 2 spontaneous interictal-like spikes (sISs) and 14 heartbeats were recorded. As indicated by the LFP, we distinguished 2 sections of the signals containing a sIS signal (in the boxes). (*B*) Thin solid line is the raw data on 1 optical detector during one of the sISs shown in *A*. Dashed line is the averaged pulsation noise of the same detector. This line was the average of pulsation noise triggered by the peak of the QRS wave in the ECG. The processed signal (thick solid line) of that sIS was obtained by subtracting the averaged pulsation from the raw data of each individual detector. The bottom two traces are the LFP and ECG traces recorded during the same sIS.

color image, the amplitude of the normalized IS signal (between 0 and 1) from each detector was assigned colors using a linear scale of 16 colors. With these color values from each detector at each data point, pseudocolor maps were made using the CONTOUR function provided by Interactive Display Language (IDL) (Research System, Boulder, CO) and used by NeuroPlex. The initiation site was defined as the one that reached the warm color (yellow or warmer colors) earlier than other regions. In some sISs, two neighboring detectors reached warm colors simultaneously, but the onset time had a slight difference. The one with the earlier onset time was defined as the initiation site.

Normalization to the spike peak amplitude on each detector was necessary before making a pseudocolor map (Fig. 3*C*). The peak amplitude of optical signals at different locations may be correlated to the unevenness in the staining and other imaging factors. Without normalization, a region with higher peak amplitude (Fig. 3*C*, *1*) but a later onset may reach the warm colors earlier than other regions with lower peak amplitude but an earlier onset (Fig. 3*C*, *3*). Normalizing all the traces to the peak of the sIS solves the problem (Fig. 3*C*, *bottom*). Since our signal-to-noise ratio was high (>10, Figs. 2 and 3), in most of the detectors normalization did not appear to increase the noise level on the detectors with small peak amplitude (e.g., Fig. 3*C*, *3*).
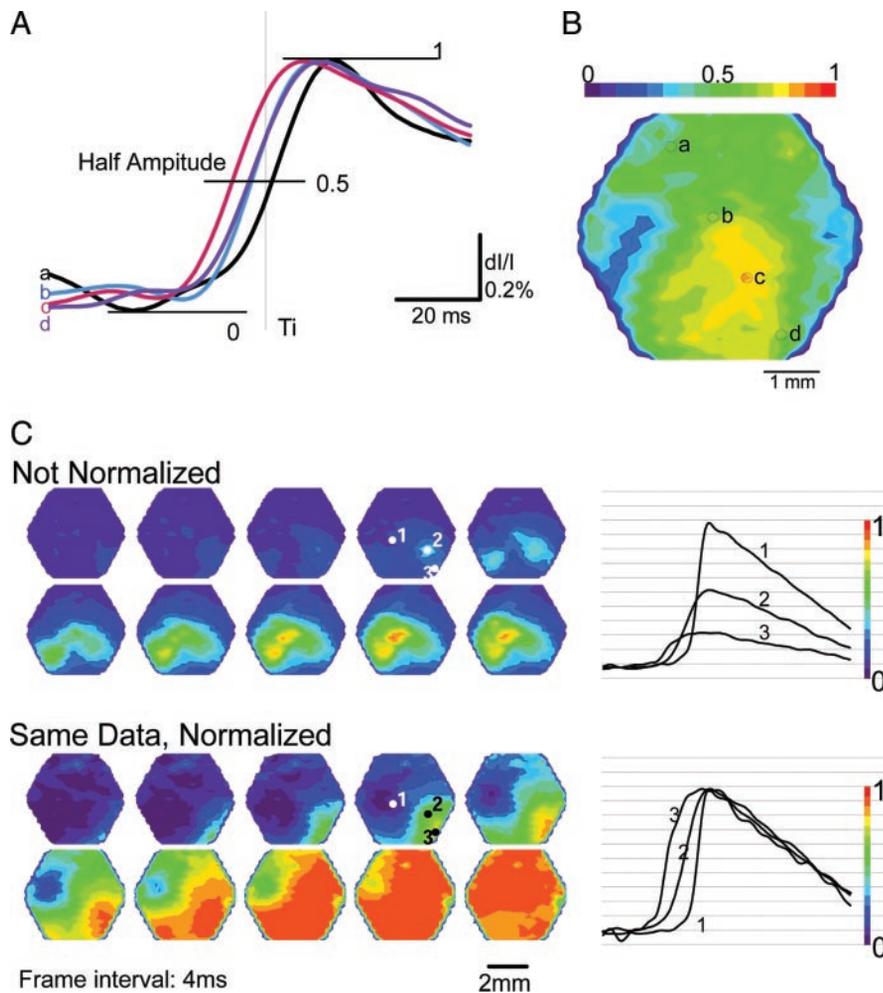
FIG. 3. *A*: processed signals (after pulsation subtraction) during a single sIS were normalized at the peak of the sIS. Four traces from 4 detectors, *a–d*, are displayed in an expanded time scale. Half-peak amplitude (0.5) is marked with a horizontal line. Locations of these detectors are marked in *B*. Signal from detector *c* had the earliest onset time, indicating that *c* was the initiation site. *B*: pseudocolor map made at time *T*i (marked by the thin line in *A*). Detector *c* had a warmer color than other regions, indicating that *c* was the initiation site; consistent with the result shown in *A*. *C*: normalization is necessary for locating the initiation site. From the same data 2 series of pseudocolor maps, normalized (*bottom*) and unnormalized (*top*) are shown. Traces from three detectors, *1–3*, are shown on the right. *Trace 3* reached half-amplitude earliest. Without normalization, signals on other detectors (e.g., *1* and *2*) reached warm colors, but the actural initiation site (detector *3*) never did. Color scale bar on the right shows how different colors were assigned to different signal amplitudes.

RESULTS

The sISs occurred several seconds after application of 1 mM bicuculline or picrotoxin to the cortex. In LFP recordings, the first several events had small and variable amplitude (0.2–0.4 mV) and irregular rates (approximately 3 Hz). The activity soon became stable, showing spikes with similar waveform and amplitude (approximately 1 mV) and lower but more stable frequency (0.3–0.75 Hz). This stable activity lasted for more than 2 h. The frequency of the sISs was higher (approximately 1.2 Hz) when the GABA$_b$ receptor antagonist CGP-35348 (1 mM) was added to bicuculline. Staining the cortex with the VSD RH-795 did not change the LFP amplitude, waveform, and frequency of the sISs. The fluorescent signal of the stained cortex had two components. One of these, which correlated well with the ECG, was apparently an artifact associated with the heartbeat. The other component, which correlated well with the sISs recorded by the LFP electrode, was presumably the VSD signal of the sISs (Fig. 2*A*). After subtracting the averaged pulsation artifact (see METHODS), the optical signal had a waveform and time course closely correlating that of the LFP recording from a nearby location (Fig. 2*B*). The waveforms of the electrical and optical recordings were not identical (Fig. 2*B*); probably because the electrical recording was affected by volume conductance effect and was triphasical (Buzsaki and Traub 1997); the VSD signal strictly reflected the membrane potential changes (Ross et al. 1977; Salzberg et al. 1973) and was not affected by the current flows in the tissue.

To identify the initiation site of the sIS, we compared the onset time of the signal recorded from different locations. In Fig. 3*A*, signal from four detectors are shown. The distance between the two detectors was 1200 μm (Fig. 3*B*). The trace recorded from detector *c* reached its half-peak amplitude earlier than other detectors, suggesting that the sIS started near detector *c* and propagated to the other locations. The pseudocolor image also showed the location of the initiation site. One image (Fig. 3*B*) was made at the time T_i (Fig. 3*A*, thin line). The orange color under detector *c* represents greater neuron excitation than other regions, demonstrating that the region under detector *c* activated earlier than the other regions. All the sISs examined optically appeared to be initiated from a small initiation site (single detector) and propagated to the whole field of view (Fig. 4*A*), suggesting that, although the entire exposed cortex was disinhibited, the sIS starts from local interactions in a small area (approximately 200 μm). This is consistent with the observations made in neocortical slices (Tsau et al. 1998, 1999) and a recent report of in vivo observations (Miyakawa et al. 2003).

Figure 4*A* shows three sISs. All the sISs started from small spots at different locations in the field of view. Sites *I* and *II* were close to each other while Site *III* was far way from *I* and *II*. All the initiation sites (26 events) recorded from this animal
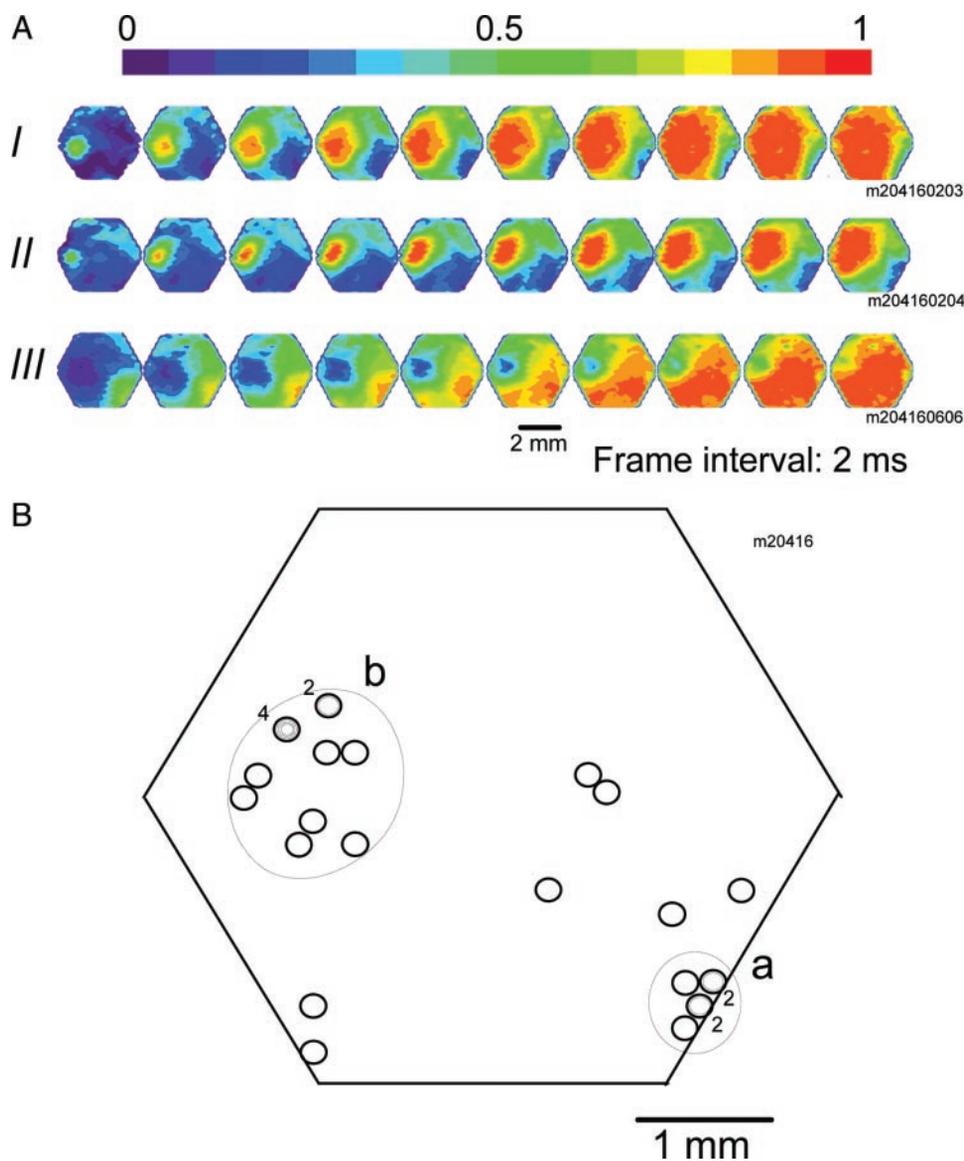
FIG. 4. *A*: three sISs initiated from different initiation sites in the same field of view. Each row of images showed the first 18 ms of a sIS. *I*: sIS initiated from the middle left of the view field; *II*: another sIS started 1.5 s later from a site near the previous initiation site; *III*: the third sIS occurred 30 min later, initiated far from the first two sites. *B*: initiation sites of 26 sISs recorded from the same animal shown in *A*. Each circle marks the location of 1 initiation site. When more than 1 sIS was initiated from the same site, smaller circles were drawn inside the circle, and the number next to the circles indicates the number of sISs initiated from that site. Note that the initiation sites were not evenly distributed in the field of view. The initiation sites appeared to be clustered in 2 areas, *a* and *b*.

are shown in Fig. 4*B*. These 26 events were started from 20 sites. In our entire data sets (9 animals), 499 sISs were initiated from 251 initiation sites, with an average of 2.0 ± 0.8 events from each site. This suggests that sIS initiation in vivo is different from that in vitro in cortical slices, where each initiation site initiated 30–100 sISs (Tsau et al. 1998). The initiation sites in Fig. 4*B* were not randomly distributed. Some sites are clustered (e.g., in areas *a* and *b* in Fig. 4*B*) and in other regions they are more scattered. This uneven distribution of initiation sites was further examined below.

Figure 5 shows the distribution of the initiation sites from six animals. Each initiation site was marked as a dot and a line was used to connect each initiation site with its predecessor. The length of the line was referred to as "shift distance," representing the distance between two successive initiation sites. The shift distances shown in Fig. 5 appeared to be either short (<800 μm) or long (>1200 μm). Of the total 94 shift distances shown in this figure, 30 (31.9%) were short and 61 (64.9%) were long. Only 3 (3.2%) of them were between 800 and 1200 μm. It appeared that surrounding each initiation site there was a "suppression annulus" within which the likelihood of starting the next sIS was reduced.

The suppression annulus became even more obvious when data from all nine animals were pooled together. In this data set we had 499 sISs and 436 shift distances. (The first initiation site of each recording trial did not have a predecessor and, therefore, had no shift distance.) Each shift distance was assigned to the initiation site after shift and the assigned initiation sites were plotted sequentially (illustrated in Fig. 6, *Ai* and *Aii*). The initiation sites were then grouped according to their shift distances. Each bin was defined by two shift distances (e.g., *S1* and *S2* in Fig. 6, *Aii*) and contained the initiation sites in an annular region defined by two radii equal to the two shift distances. In a simulated data set where the initiation sites were randomly distributed in space (Fig. 6*B*, *i*), the number of initiation sites increased with the size of the annulus (Fig. 6*B*, *ii*), but the density of the sites in each bin (number of initiation sites divided by the area of the annulus) remained constant (Fig. 6*B*, *iii*). Figure 6*C* shows the density curve of the observed data (thick line) and the simulated data (dotted line). In the observed data, the densities of the 2 bins at 0–200 and 200–400 μm were significantly higher than the simulated data, suggesting a clustering effect of the initiation sites in a circular
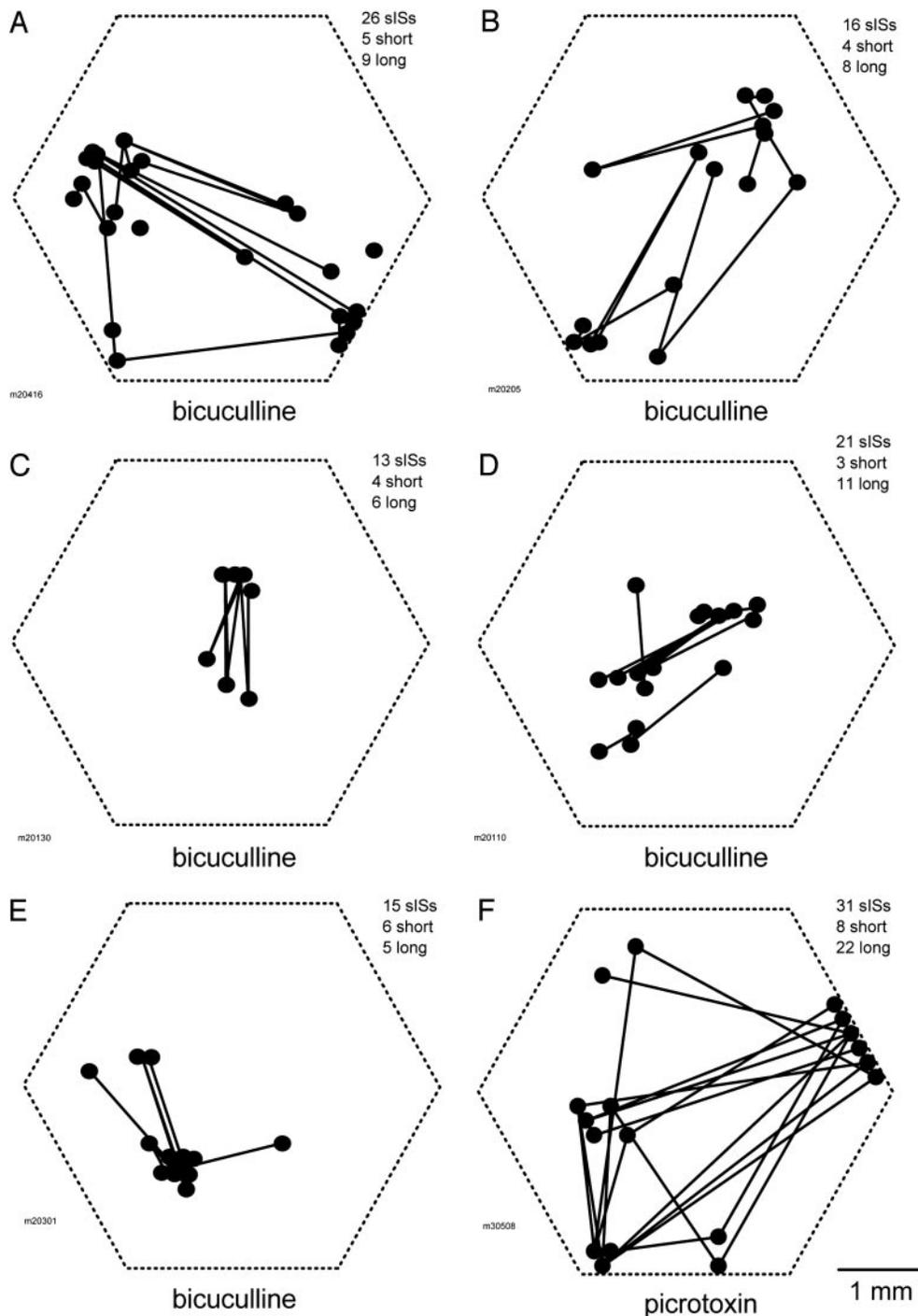
FIG. 5. Shifting of initiation sites. *A–F*: measurements from 6 animals. Each dot marks the location of an initiation site. The lines connect the initiation sites of consecutive sISs. The length of the lines is referred to as the shift distance. On the upper right corner of each panel (from *top* to *bottom*) the number of sISs recorded from this field of view, the number of lines with short (<800 μm), and long (>1200 μm) shift distances is listed. *A–E*: sISs were induced with 1 mM bicuculline. *F*: sISs were induced with 1 mM picrotoxin. There were 116 sISs recorded from this preparation but only 31 were shown, for better clarity.

area of 0–400 μm surrounding each initiation site. The difference among the rest of nine bins (in the region of 400-2200 μm surrounding each initiation site) was tested by ANOVA with the Bonferroni post-hoc test. The densities in the 800–1000 μm and 1000–1200 μm bins were not significantly different from each other but were significantly lower than the three neighboring bins of 400–600, 600–800, and 1200–1400 μm (Table 1, *asterisks*), suggesting a local minimum in the region

of 800–1200 μm. A *t*-test was used to individually compare the 800–1000 or the 1000–1200 bins to the rest of the other bins. The test result confirmed that both bins in the local minimum had a significantly lower density than any other bins ($P < 0.05$).

The *t*-test also showed that the densities of the 800–1000 and the 1000–1200 μm bins were significantly lower than those of the simulated data ($P < 0.01$). The low densities in

these two bins supported the existence of the suppression annulus between the radii of 800-1200 μm.

We also used a surrogate of the observed data to further verify the existence of the suppression annulus. In the surro-

gate we randomized the temporal sequence of the sISs and the shift distances were measured from all possible combinations of the initiation sites in each animal (e.g., if one animal yielded 10 sites, 45 shift distances could be measured). The surrogate
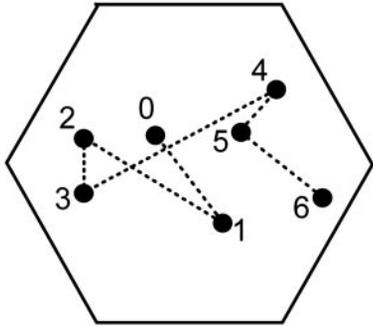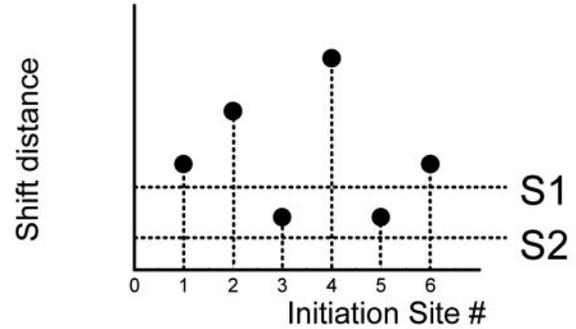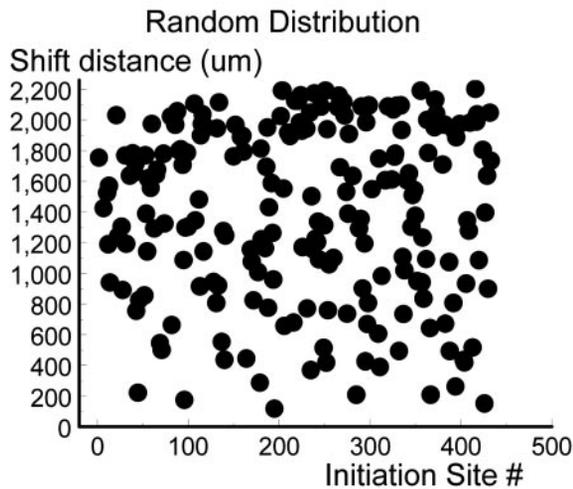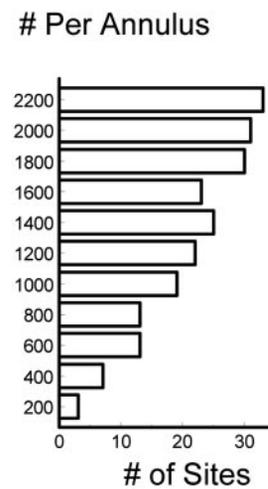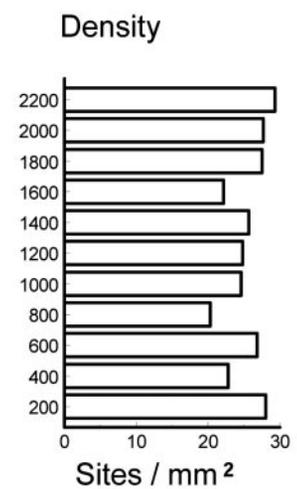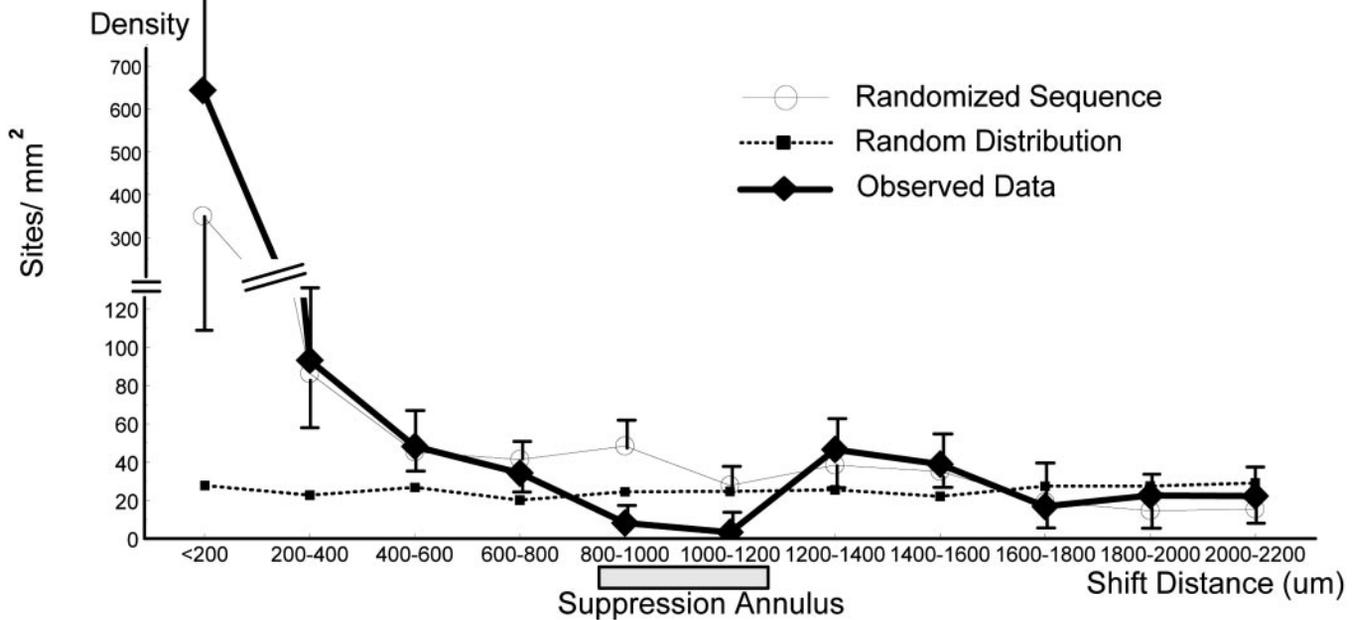
contained 1260 shift distances. We divided the density of the surrogate data by a factor of 2.89 (1260/436 = 2.89), so that the surrogate (Fig. 6*C*, thin line) could be directly compared with the observed data. In the surrogate the clustering between 0 and 400 μm was obvious but the local minimum in the range of 800–1200 μm disappeared. The difference between the observed data and the surrogate was significant in the 800-1200 μm region (*t*-test, *P* < 0.01) while not in other regions (200–800 μm and 1400–2200 μm; *t*-test, *P* > 0.05). This comparison further confirmed that the likelihood for initiating the next sIS was reduced in the suppression annulus; it also indicated that the suppression only occurred temporarily, affecting only the initiation of the next sIS.

The synaptic mechanisms of suppression annulus were tentatively explored. In the presence of high concentration of bicuculline, the calcium-activated potassium channels may be partially blocked (Strobaek et al. 2000). To eliminate this effect, picrotoxin was used instead of bicuculline. The suppression annulus still appeared in the picrotoxin bath (Fig. 7), suggesting that the suppression annulus was not a result of K^+ channel blockade. GABA$_b$ antagonist CGP35348 was used together with bicuculline to test whether the suppression annulus was a result of the GABA$_b$-mediated inhibition. In the presence of CGP35348 the occurrence rate of the sISs increased (approximately 1.2 Hz). However, the distribution of the initiation sites did not show any significant difference from that with bicuculline alone (Fig. 7), suggesting that GABA$_b$ inhibition was not involved.

In an effort to see whether the distribution of the initiation sites was correlated to the spatial distribution of local neuronal activity, we applied bicuculline to the cortex locally before the entire exposed cortex was disinhibited by bicuculline. A small piece of filter paper (approximately 800 × 800 μm^2) soaked with 1 mM bicuculline was placed on the cortex for approximately 45 min. During this period about 1000 sISs were recorded from this local area with a LFP electrode. Optical imaging showed these sISs could not be detected outside of the region of bicuculline application (data not shown). Bicuculline or picrotoxin (1 mM) was then applied to the entire exposed cortex for an additional 45 min and imaging was carried out during this period. The sISs were recorded from the entire field of view (Fig. 8*A*), but many initiation sites were clustered near the filter paper (Fig. 8*B*). In one animal, 17 of 33 sISs were initiated near the filter paper (Fig. 8*B*, *2*). This suggests that the chance to initiate a sIS increased in the area with bicuculline pretreatment. It is possible that the approximately 1000 sISs in the pretreatment area modified the local network, which thus created the clustering of initiation sites.

Again we saw a suppression annulus surrounding the initiation site. Because the pretreatment created a cluster of initiation sites near the filter paper, the suppression annulus can be seen in the results from individual animals (Fig. 8*B*, *1–4*). Of the total of 310 sISs recorded in six animals, 135 (43.6%) initiated from the region within 800 μm from the filter paper; 11 (3.5%) initiated in the region between 800 to 1200 μm from the filter paper (suppression annulus), and 164 (52.9%) initiated from outside of the suppression annulus (>1200 μm). The distribution of the initiation sites was shown in Fig. 8*C* (the distance between the initiation sites and the edge of the filter paper was used as the shift distance). A local minimum between 800 and 1200 μm occurred in the distribution, indicating the existence of suppression annulus.

DISCUSSION

Differences between in vivo and in vitro

In this report we have observed 499 sISs from 251 sites, or each initiation site initiated about two epileptiform events. This is very different from our previous observations in brain slices where each site initiated 30–100 events (300–400 events from 3–4 sites; Tsau et al. 1998). Several factors might contribute to this difference: first, an intact cortex contains more tissue than a slice and thus contains more potential initiation sites. Second, a brain slice is only a small vertical section of the cortical network and horizontal connections are largely cut. Horizontal connections may promote interactions for sIS initiation. Third, under in vivo conditions, cortical neurons may have higher levels of spontaneous activity, which may trigger sISs. In a neocortical local network, if only a few groups of neurons have a certain level of spontaneous activity that can trigger an IS, then all the sISs would start from these few initiation sites and each initiation site would initiate many sISs. In contrast, if many neurons have high levels of spontaneous activity that can trigger an IS, then sISs would start from many possible sites and each initiation site would initiate only a few sISs, as seen in this report.

Synchronized firing of a local neuronal population may be required for the initiation of an IS (Demir et al. 1999; Jefferys 1990; Jensen and Yaari 1997). It is well known that an evoked activity from an electrical shock to a rat neocortex slice can reliably trigger an IS (Chagnac-Amitai and Connors 1989; Curtis et al. 1970; Prince 1967). In intact cortex, evoked activity by deflection of a whisker can also reliably trigger the initiation of an IS (London et al. 1989; Prince 1966). These evoked activities are all visible in LFP electrode recordings, suggesting a certain level of synchrony within the local neuronal population. Bathed in normal ACSF, in vitro slices showed no obvious spontaneous activity in LFP recordings. In contrast, EEG recordings from anesthetized rat cortex showed constant spontaneous activity, suggesting that there were more possible triggers for starting sIS in vivo.

FIG. 6.   Spatial distribution of the initiation sites. *A* and *B*: method for grouping the initiation sites according to their shift distances. *Ai*: seven initiation sites (1–7) are connected by 6 shift distances (dotted lines). Each shift distance was assigned to the initiation site after shift. *Aii*: assigned initiation sites (1–6) were plotted according to their shift distances and appearing sequence. *S1* and *S2* illustrate the lower and upper border of each bin. *Bi*: same plot for a simulated data set of 436 randomly distributed initiation sites. Drop lines were omitted for the sake of clarity. *Bii*: histogram of number of initiation sites according to shift distance, binwidth 200 μm. *Biii*: density histogram of the initiation sites (number of initiation sites in each annulus divided by the area of the annulus). *C*: densities of observed data (436 shift distances, thick line), the surrogate data (thin line), and simulated data of random distribution (436 shift distances, dotted line) in each bin. The observed data and its surrogate were averaged over 9 animals. Error bar represents SE.

TABLE 1. *Bonferroni post-hoc test with nine data bins*

P Value	400–600 μm	600–800 μm	800–1000 μm	1000–1200 μm	1200–1400 μm	1400–1600 μm	1600–1800 μm	1800–2000 μm	2000–2200 μm
400–600 μm	—								
600–800 μm	1.000	—							
800–1000 μm	0.007*	0.049*	—						
1000–1200 μm	0.003*	0.022*	1.000	—					
1200–1400 μm	1.000	1.000	0.048*	0.020*	—				
1400–1600 μm	1.000	1.000	0.505	0.229	1.000	—			
1600–1800 μm	0.108	1.000	1.000	1.000	0.602	1.000	—		
1800–2000 μm	0.624	1.000	1.000	1.000	1.000	1.000	1.000	—	
2000–2200 μm	0.703	1.000	1.000	1.000	1.000	1.000	1.000	1.000	—

* Significant difference between two bins ($P < 0.05$).

Number of initiation sites

Our observation of the spatial distribution of the initiation sites did not agree with Miyakawa et al. (2003). They observed only 2 to 4 initiation sites in each animal (Fig. 6 of Miyakawa et al. 2003). This was significantly fewer than our observations of 7–35 initiation sites per animal but somewhat similar to that observed in brain slices (Tsau et al. 1998).

We postulated that different ways of defining initiation sites might contribute to this discrepancy. In the two methods used in this report (Fig. 3), both defined an initiation site as a location where the signal first reached half of normalized peak amplitude. In contrast, Miyakawa et al. (2003) defined the initiation site as a position in which the signal first reached a threshold (of S/N > 2). With their method, a location with higher signal amplitude (also higher signal-to-noise ratio) may

reach the threshold earlier, even though its onset time was later than other locations (e.g., Fig. 3C, top, detector 2). Since signal size may be related to the staining and other imaging factors, the location of the initiation site might also be biased.

Suppression annulus

The suppression annulus was not in the immediate surrounding region of each initiation site. Rather, it started some distance (approximately 800 μm) away from an initiation site (Fig. 6C, 7). Thus the area immediately surrounding the initiation center may host initiation sites for the next sIS, creating a cluster effect. This clustering effect was more obvious when the preparation was pretreated with a local application of bicuculline (Fig. 8, B and C). The pretreatment of applying bicuculline locally promotes multiple initiation sites in a small
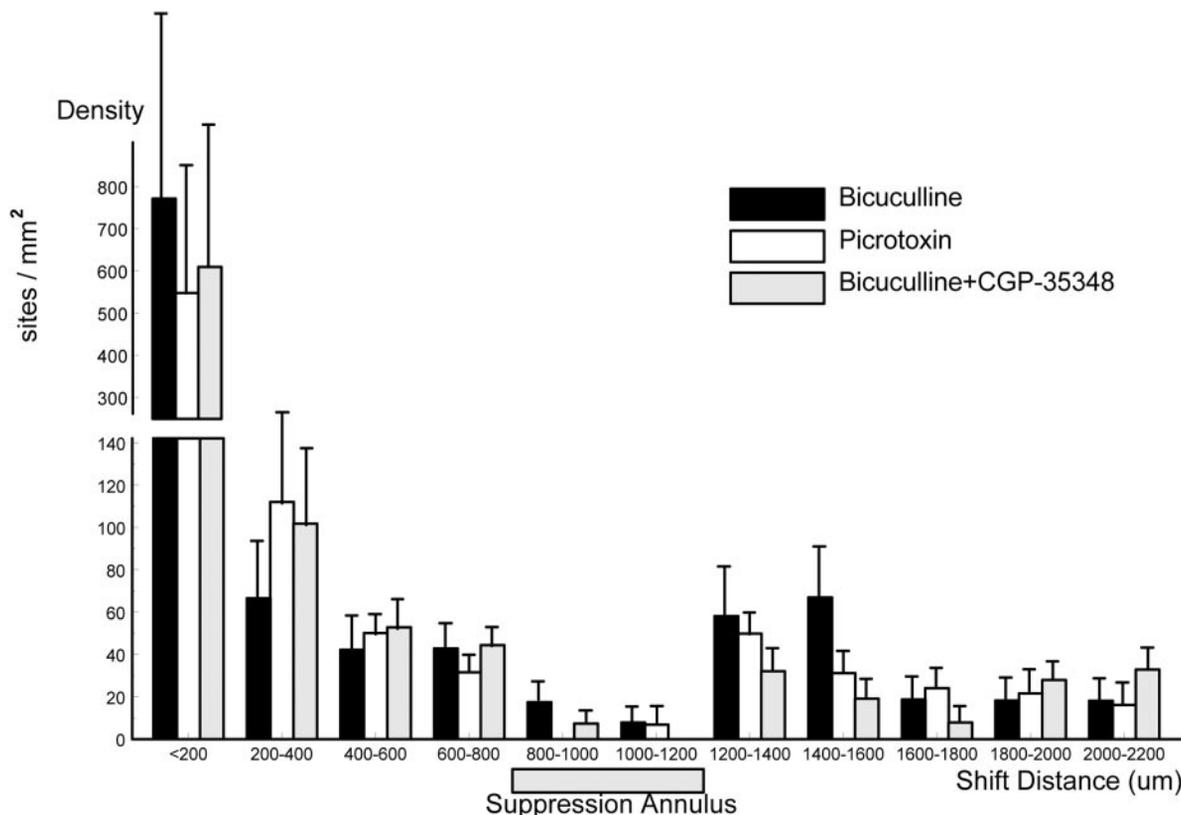

FIG. 7. Density histogram of the initiation sites induced by bicuculline (1 mM), picrotoxin (1 mM), and bicuculline (1 mM) + CGP-35348 (1 mM). The three conditions were normalized to their number of initiation sites to facilitate a direct comparison. In all three conditions the clustering and suppression annulus were similar.
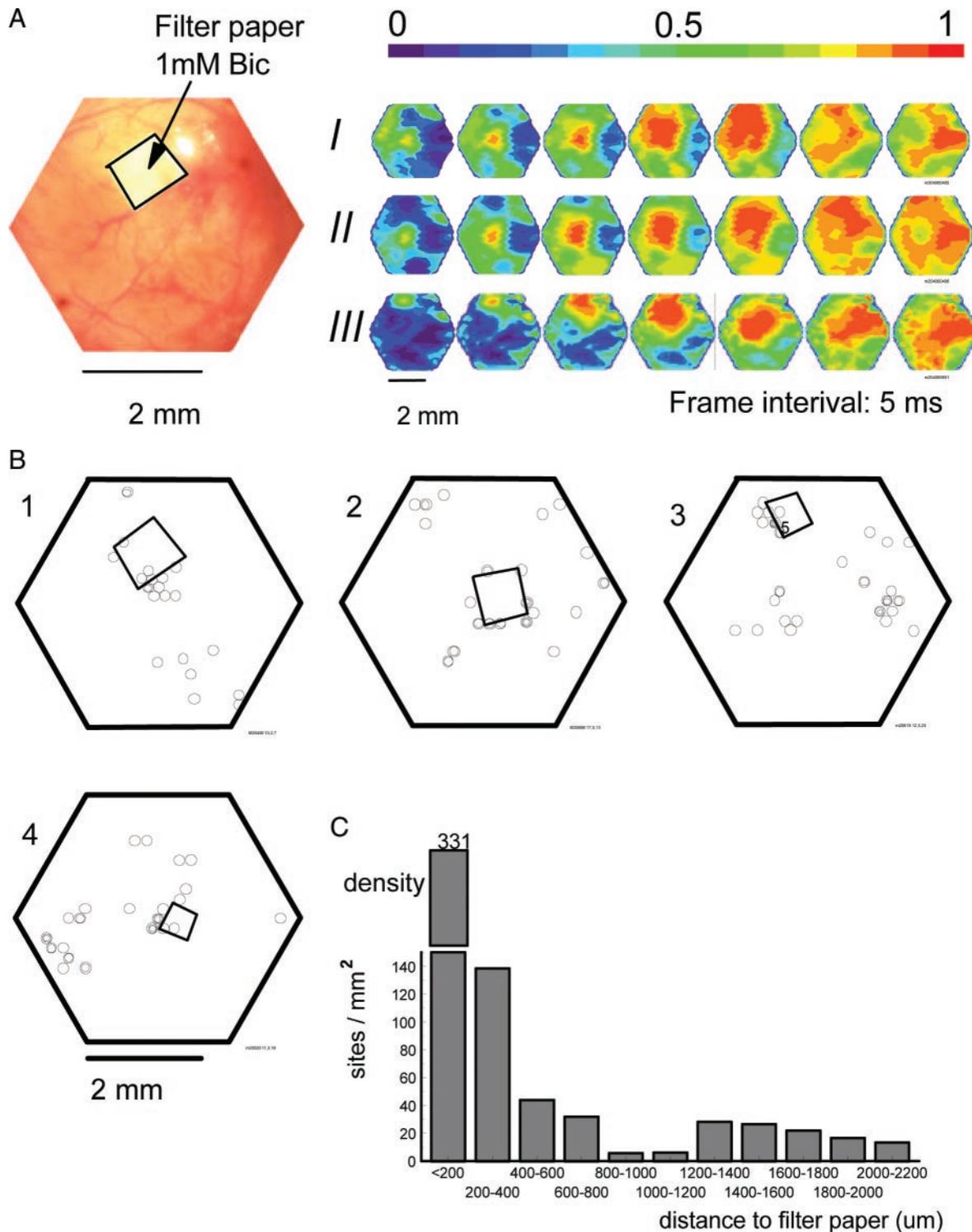
FIG. 8. Effect of bicuculline pretreatment. *A*: image on the left shows the field of view and the bicuculline-soaked filter paper. Pseudocolor images on the right are 3 sISs recorded from this field of view. Events *I* and *II* initiated near the filter paper, and *III* initiated approximately 1100 μm away. *B*: sIS initiation sites of 4 animals. Many initiation sites were clustered around the filter paper. *B1* is from the same animal as that shown in *A*. *C*: density plot. Initiation sites were grouped according to their distance to the edge of the filter paper. The high density at 0–400 μm and the local minimum between 800 and 1200 indicated the clustering and the suppression annulus.

area and the suppression annulus for the clustered initiation sites may overlap and was, therefore, visible in individual preparations.

The mechanism that might underlie the suppression annulus was only tentatively explored. A possible involvement of $GABA_b$ inhibition was excluded. However, the occurring rate of sIS increased in the presence of $GABA_b$ antagonist, suggesting that $GABA_b$ inhibition contributes to the regulation of

the sISs occurring rate. The underlying mechanisms of the temporal suppression will be further investigated.

sIS is an all-or-none event and it propagates over the entire cortical area that is exposed to bicuculline or picrotoxin. Thus one might think that the location of the initiation site should not affect the activity in other areas. Timing would be the only difference between the activity at the initiation site and the rest of the regions. It is, therefore, difficult to speculate about a network mechanism that would explain the phenomenon of the suppression annulus. In addition, the suppression annulus occurred only briefly (within a few seconds) after each sIS, adding difficulties for further study.

The existence of an "inhibitory surround" in the cortex adjacent to an acute artificial epilepsy focus has been previously suggested by a number of authors. An electrophysiological inhibitory surround was demonstrated with a single-unit recording from the cortex adjacent to acute experimental foci (Goldensohn and Salazar 1986; Prince and Wilder 1967). Negative signals were also recorded with interictal PET, fMRI, SPECT, and optical recordings based on intrinsic signals (Federico et al. 1994; Schwartz and Bonhoeffer 2001). The inhibitory surround mentioned by these authors was induced with locally applied convulsants. Within the area of inhibitory surround the $GABA_a$ inhibition was not suppressed. In this report, bicuculline is applied to the entire explored cortex and in the suppression annulus the $GABA_a$ inhibition was blocked. These suggest that the inhibitory surround and suppression annulus are two different phenomena; additional experiments are required to examine their correlations. In addition the suppression annulus in this report did not block propagation of sISs. It only reduced the chance for initiating the next sIS in the annulus. The inhibitory surround, in contrast, blocks the IS propagation.

We estimated that the width of the suppression annulus was about 400 μm (Fig. 6C). At least two factors could affect the accuracy of this estimation. The first was the spatial resolution of our imaging setup, which was about 200 μm. The second was the individual variability. The local minimum in Fig. 6C was an average of our entire data set. Using the current methods we were unable to detect the actual size of the suppression annulus surrounding each individual initiation site. Despite the inaccuracy, the existence of the suppression annulus must be real, because the probability of sISs initiation was significantly lower in the annulus than its neighboring areas. This local minimum of the curve could not be eliminated when the grouping of the initiation sites was varied (e.g., from groups of 600–800, 800–1000, and 1000–1200. . . to groups of 500–700, 700–900, and 900–1100 μm. . . etc.; data not shown).

We speculate that the size of the suppression annulus might be related to the geometry of arborizations of dendrites and axons of cortical neurons. Although the long-range inhibitory connections (e.g., by large basket cells, Somogyi et al. 1983; Kisvarday et al. 1986) are greatly reduced when the $GABA_a$ inhibition is blocked, other short and long range connections might be related (e.g., the clustering and long range corticocortical projections of infragranular pyramidal cells, Martin and Whitteridge 1984; Szentágothai 1987). Additional studies are needed to explore the correlation between the boundaries of the suppression annulus (800–1200 μm) and anatomical connectivity.

Clustering of initiation sites and activity history

A cluster of sIS initiation sites can be created by locally applying bicuculline to the cortex before disinhibiting a large area (Fig. 8). The bicuculline concentration at the local area was the same as that later applied to the entire craniotomy window. The local area was exposed to bicuculline approximately 45 min earlier than the rest of the cortical area. During the period of local bicuculline pretreatment, about 1000 sISs occurred in that area. These activities may modify the cortical network in that small region and the modification may play a role in promoting the initiation sites. In six different animals we applied the pretreatment on different cortical regions but the cluster was always formed around the filter paper, suggesting that the cluster was linked to the pretreatment and unlikely to be associated any particular cortical areas. However, cortex is not a homogenous tissue and we expect the heterogeneity in the local network would also contribute to the formation of clustering and suppression annulus. A future direction would be to examine the distribution of clusters due to heterogeneity and how the altered local activity would modify the "intrinsic" distribution.

VSD method

VSD imaging provided a convenient way to map the initiation of epileptiform activity in the cortex. The dye signal of epileptiform activity is large (Demir et al. 1999; London et al. 1989; Jin et al. 2002), yielding a high signal-to-noise ratio without averaging. Seeing activity without averaging is important for examining the variant initiation and spatial–temporal dynamics of epileptiform activities.

A major drawback of the dye RH-795 is the large heartbeat artifact in the optical recordings, due to the excitation wavelength of the dye overlapping with the absorption band of hemoglobin (Shoham et al. 1999). Our method for subtracting the cardiovascular artifact was not perfect, because each individual heartbeat varies and subtracting the average left residuals. However, since the IS signal is large, the subtraction method seems adequate. A new generation of VSDs is being developed (Shoham et al. 1999). These dyes have an excitation wavelength that does not overlap with the hemoglobin absorption (the "blue dyes"). The heartbeat artifact is thus significantly reduced (Shoham et al. 1999).

In conclusion, we found that the distribution of sIS initiation sites in the intact cortex is different from that found in cortical slices; there are multiple initiation sites in the intact cortex and each site initiates only a few sISs. The initiation sites are not evenly distributed. Increased local activity may create a cluster of initiation sites. Around each initiation site there appears to be a temporal suppression annulus, where the chance of initiating the next sIS was reduced. However, we did not examine the correlation between the cellular architecture and the location of the clusters. Also our pharmacological manipulations did not verify the existence of a suppression annulus. Additional experiments are needed to work in these directions.

REFERENCES

Ajmone MC. Clinical electrographic correlation of partial seizures. In: *Modern Perspectives in Epilepsy*, edited by Wada JA. Proceedings of the Inaugural Symposium of the Canadian League Against Epilepsy. Montreal: Eden Press, 1978, p. 76–98.

Anderson WW, Lewis DV, Swartzwelder HS, and Wilson WA. Magnesium-free medium activates seizure-like events in the rat hippocampal slice. *Brain Res* 398: 215–219, 1986.

Bonhoeffer T and Grinvald A. In: *Brain Mapping. The Method* edited by AW Toga and JC Mazziota JC. San Diego, CA: Academic, 1996, p. 55–99.

Buzsáki G and Traub RD. Generation of EEG. In: *Epilepsy: A Comprehensive Textbook,* edited by J Engel Jr. and TA Pedley. Philadelphia: Lippincott-Raven Press 1997, p. 819–830.

Chagnac-Amitai Y and Connors BW. Synchronized excitation and inhibition driven by intrinsically bursting neurons in neocortex. *J Neurophysiol* 62: 1149–1162, 1989.

Cohen LB and Salzberg BM. Optical measurement of membrane potential. *Rev Physiol Biochem Pharmacol* 83: 35–88, 1978.

Curtis DR, Duggan AW, Felix D, and Johnston GA. GABA, bicuculline and central inhibition. *Nature* 226: 1222–1224, 1970.

Demir R, Haberly LB, and Jackson MB. Sustained and accelerating activity at two discrete sites generate epileptiform discharges in slices of piriform cortex. *J Neurosci* 19: 1294–1306, 1999.

Duncan JS. Imaging and epilepsy. *Brain* 120: 339–377, 1997.

Federico P, Borg SG, Salkauskus AG, and MacVicar BA. Mapping patterns of neuronal activity and seizure propagation by imaging intrinsic optical signals in the isolated whole brain of the guinea-pig. *Neuroscience* 58: 416–480, 1994.

Flint AC and Connors BW. Two types of network oscillations in neocortex mediated by distinct glutamate receptor subtypes and neuronal populations. *J Neurophysiol* 75: 951–957, 1996.

Goldensohn ES and Salazar AM. Temporal and spatial distribution of intracellular potentials during generation and spread of epileptogenic discharges. *Adv Neurol* 44: 559–582, 1986.

Grinvald A, Lieke EE, Frostig RD, and Hildesheim R. Cortical point-spread function and long-range lateral interactions revealed by real-time optical imaging of macaque monkey primary visual cortex. *J Neurosci* 14: 2545–2568, 1994.

Jefferys JG. Basic mechanisms of focal epilepsies. *Exp Physiol* 75: 127–162, 1990.

Jensen MS and Yaari Y. Role of intrinsic burst firing, potassium accumulation, and electrical coupling in the elevated potassium model of hippocampal epilepsy. *J Neurophysiol* 77: 1224–1233, 1997.

Jin W, Zhang RJ, and Wu JY. Voltage-sensitive dye imaging of population neuronal activity in cortical tissue. *J Neurosci Methods* 115: 13–27, 2002.

Kisvarday ZF, Martin KA, Freund TF, Magloczky Z, Whitteridge D, and Somogyi P. Synaptic targets of HRP-filled layer III pyramidal cells in the cat striate cortex. *Exp Brain Res* 64: 541–552, 1986.

Lebovitz RM. Effects of temperature on interictal discharge at penicillin epileptogenic foci. *Epilepsia* 16: 215–22, 1975.

Lieke EE, Frostig RD, Arieli A, Ts'o DY, Hildesheim R, and Grinvald A. Optical imaging of cortical activity: real-time imaging using extrinsic dye-signals and high resolution imaging based on slow intrinsic-signals. *Annu Rev Physiol* 51: 543–559, 1989.

London JA, Cohen LB, and Wu JY. The spread of epileptiform discharges in the somatosensory cortex of the rat measured with voltage sensitive dyes. *J Neurosci* 9: 2182–2190, 1989.

Martin KA and Whitteridge D. Form, function and intracortical projections of spiny neurones in the striate visual cortex of the cat. *J Physiol* 353: 463–504, 1984.

McCormick DA and Contreras D. On the cellular and network bases of epileptic seizures. *Annu Rev Physiol* 63: 815–846, 2001.

McNamara JO. Cellular and molecular basis of epilepsy. *J Neurosci* 14: 3413–3425, 1994.

Miyakawa N, Yazawa I, Sasaki S, Momose-Sato Y, and Sato K. Optical analysis of acute spontaneous epileptiform discharges in the *in vivo* rat cerebral cortex. *NeuroImage* 18: 622–632, 2003.

Prince DA. Modification of focal cortical epileptogenic discharge by afferent influences. *Epilepsia* 7: 181–201, 1966.

Prince DA. Electrophysiology of "epileptic neurons." *Electroencephalogr Clin Neurophysiol* 23: 83–84, 1967.

Prince DA and Wilder BJ. Control mechanisms in cortical epileptogenic foci. "Surround" inhibition. *Arch Neurol* 16: 194–202, 1967.

Ross WN, Salzberg BM, Cohen LB, Grinvald A, Davila HV, Waggoner AS, and Wang CH. Changes in absorption, fluorescence, dichroism, and Birefringence in stained giant axons: optical measurement of membrane potential. *J Membr Biol* 33: 141–183, 1977.

Salzberg BM, Davila HV, and Cohen LB. Optical recording of impulses in individual neurones of an invertebrate central nervous system. *Nature* 246: 508–509, 1973.

Schwartz TH and Bonhoeffer T. *In vivo* optical mapping of epileptic foci and surround inhibition in ferret cerebral cortex. *Nat Med* 7: 1063–1067, 2001.

Shoham D, Glaser DE, Arieli A, Kenet T, Wijnbergen C, Toledo Y, Hildesheim R, and Grinvald A. Imaging cortical dynamics at high spatial and temporal resolution with novel blue voltage-sensitive dyes. *Neuron* 24: 791–802, 1999.

Silva LR, Amitai Y, and Connors BW. Intrinsic oscillations of neocortex generated by layer 5 pyramidal neurons. *Science* 251: 432–435, 1991.

Somogyi P, Kisvarday ZF, Martin KA, and Whitteridge D. Synaptic connections of morphologically identified and physiologically characterized large basket cells in the striate cortex of cat. *Neuroscience* 10: 261–294, 1983.

Strobaek D, Jorgensen TD, Christophersen P, Ahring PK, and Olesen SP. Pharmacological characterization of small-conductance $Ca(2+)$-activated $K(+)$ channels stably expressed in HEK 293 cells. *Br J Pharmacol* 129: 991–999, 2000.

Szentágothai J. (1987) The architecture of neural centres and understanding neural organization. In: *Advances in Physiological Research,* edited by H. McLennan, JR Ledsome, CHS McIntosh, and DR. Jones. New York: Plenum, p. 111–131.

Takashima I, Ichikawa M, and Iijima T. High-speed CCD imaging system for monitoring neural activity *in vivo* and *in vitro*, using a voltage-sensitive dye. *J Neurosci Methods* 91: 147–159, 1999.

Traub RD, Jefferys JG, and Whittington MA. Enhanced NMDA conductance can account for epileptiform activity induced by low Mg^{2+} in the rat hippocampal slice. *J Physiol* 3: 379–393, 1994.

Tsau Y, Guan L, and Wu JY. Initiation of spontaneous epileptiform activity in the neocortical slice. *J Neurophysiol* 80: 978–982, 1998.

Tsau Y, Guan L, and Wu JY. Epileptiform activity can be initiated in various neocortical layers: an optical imaging study. *J Neurophysiol* 82: 1965–1973, 1999.

Wong BY and Prince DA. The lateral spread of ictal discharges in neocortical brain slice. *Epilepsy Res* 7: 29–39, 1990.

Wu JY and Cohen LB. Fast multisite optical measurement of membrane potential. In: *Fluorescent and Luminescent Probes for Biological Activity,* edited by WT Mason. London: Academic, 1993, p. 389–404.